Journal of Radiation Research, Vol. 57, No. 2, 2016, pp. 189–200
doi: 10.1093/jrr/rrv075
Advance Access Publication: 28 December 2015

Efficacy of polysaccharide from *Alcaligenes xylosoxidans* MSA3 administration as protection against γ-radiation in female rats

Amal I. Hassan[1]*, Mona A. M. Ghoneim[1], Manal G. Mahmoud[2], Mohsen M. S. Asker[2] and Saher S. Mohamed[2]

[1]Department of Radioisotopes, Nuclear Research Centre, Atomic Energy Authority, Egypt
[2]Microbial Biotechnology Department, National Research Centre, 33 Bohouth Street, Dokki, Giza, 12311, Egypt
*Corresponding author. Department of Radioisotopes, Nuclear Research Centre, Atomic Energy Authority, Egypt. Tel.: +-2 1112900054; Fax: 4872778; Email: aml_h@hotmail.com
Received April 28, 2015; Revised August 27, 2015; Accepted September 4, 2015

ABSTRACT

Damage to normal tissues is a consequence of both therapeutic and accidental exposures to ionizing radiation. A water-soluble heteropolysaccharide called AXEPS, composed of glucose, galactose, rhamnose and glucouronic acid in a molar ratio of nearly 1.0:1.6:0.4:2.3, respectively, was isolated from culture medium of strain *Alcaligenes xylosoxidans* MSA3 by ethanol precipitation followed by freeze-drying. Chemical analysis, Fourier-transform infrared (FTIR) and chromatographic studies revealed that the molecular weight was 1.6×10^4 g mol^{-1}. This study was designed to investigate the radioprotective and biological effects of AXEPS in alleviating the toxicity of ionizing radiation in female albino rats. A total of 32 female albino rats were divided into four groups. In the control group, rats were administered vehicle by tube for four weeks. The second group was administered AXEPS (100 mg/kg) orally by gavage for four weeks. Animals in the third group were exposed to whole-body γ-rays (5 Gy) and remained for 2 weeks without treatment. The fourth group received AXEPS (100 mg/kg) orally by gavage for two weeks before being exposed to whole-body γ-rays (5 Gy), then 24 h post γ-rays, they received AXEPS (100 mg/kg) in a treatment continuing till the end of the experiment (15 days after the whole–body γ-irradiation). Oral administration of AXEPS (100 mg/kg) significantly reversed the oxidative stress effects of radiation, as evidenced by the decrease in DNA damage in the bone marrow. Assessment of apoptosis and cell proliferation markers revealed that caspase-3 significantly increased in the irradiated group. Moreover, a significant decrease in the hematological constituents of peripheral blood, the chemotactic index and CD8+ T cells were observed in animals in the irradiation-only group, whereas an increase in the lymphocyte index was observed in animals in that group. In contrast, AXEPS treatment prevented these alterations. From our results, we conclude that AXEPS is a potent antioxidant and treatment agent for protection from γ-rays.

KEYWORDS: *Alcaligenes xylosoxidans*, γ rays, polysaccharide, chemical structure, oxidative stress

INTRODUCTION

Radiotherapy, one of the most important cancer treatment modalities, relies on the generation and use of reactive oxygen species (ROS) to eradicate tumors [1]; in the process, non-target tissues are also damaged. It is well known that exposure of normal tissue cells to ionizing radiation (IR) activates genetic cascades of signaling events, generating free radicals collectively known as ROS, which can produce single- and double-strand breaks in DNA, ultimately leading to cell death. Due to the increased utilization of IR in daily life and the growing threat of global terrorism, IR-induced normal tissue morbidities are of great importance to both civilian and military populations, since they are potentially subject to accidental or intentional nuclear mishaps. Hence, the development of an efficacious radioprotector would be a valuable contribution to radiation oncology, public health, national defense, and environmental remediation [2]. Recently, the search for more effective radioprotectors has been

intensified due to increased use of IR in radiotherapy for the treatment of malignant tumors. After exposure of mammalian cells to IR, unregulated production of ROS (associated with a shift in the intracellular oxidant–antioxidant balance toward a pro-oxidant state) triggers damage to cellular membranes and DNA, leading to a state of oxidative stress. However, because effective antioxidants are free-radical scavengers that interfere with radical chain reactions, the potential is there to protect cellular DNA from oxidative stress by supplementation with antioxidants [3]. Natural products such as herbal medicines with an abundance of antioxidant resources have received attention as promising radiation modifiers [4]. Investigations show that polysaccharides from microorganisms like fungi, bacteria and algae have many biological activities, such as antioxidant activity [2, 5], antitumor activity [6], and immunomodulatory activity [7, 8]. Welan gum is an anionic exopolysaccharide (EPS) produced *by Alcaligenes* spp. [9, 10]. It is composed of tetra repeating units of glucose, rhamnose and glucuronic acid at a ratio of 2:1:1, respectively [11]. Welan gum has been improved by breeding high-producing strains and by optimizing the culture conditions [12–14]. In our study, a heterogeneous polysaccharide named 'AXEPS' was obtained and identified from *A. xylosoxidans* MSA3. The chemical characteristics of AXEPS were determined, in particular its ability to specifically inhibit the cytotoxicity induced by γ rays.

MATERIALS AND METHODS

In vitro experiments

Collection samples

Marine sediment samples (5 g) were collected from Sidi bisher (Alexandria, Egypt). The collected samples were placed in sterile bags and brought to the laboratory. These samples were stored at 4°C for later use.

Isolation of bacterial strains

The sequent dilution of the collected sample was carried out by adding 1 g of sediment to 10 ml of sterile distilled water. From this suspension, sequent dilution was performed and from that 10^{-4} and 10^{-5} dilutions were spread on marine nutrient agar plates. After incubation at 37°C for 72 h, a cultural logogriphic bacterial colony was obtained. Then colonies were isolated from each plate and subcultured on marine nutrient agar medium until pure isolates were obtained. Pure colonies of each facultative logographic isolate (capable of forming mucous and ropy colonies) were then inoculated into 50 ml of screening marine nutrient medium in 250-ml conical flasks, and incubated at 37°C in a rotary shaker at 120 rpm for 48 h. After centrifugation at 5000 rpm for 30 min, the supernatant was mixed with four volumes of chilled ethanol. The precipitate was collected by centrifugation at 5000 rpm for 30 min and the pellets were dried at 40°C under vacuum. EPS production was determined by quantifying the carbohydrate content of the pellets as glucose equivalents using the phenol–sulfuric acid method [15]. Strain NRC-47, which produces large amounts of EPS, was identified based on biochemical, morphological and physiological characteristics of the potential producer as determined by adopting standard methods [16, 17].

Characterization of selected strain by 16S rRNA

The bacteria was characterized and identified by 16S rRNA gene sequencing using universal primers ITS1-5′TCCGTAGGTGAAC TTTGCGG3′ and ITS4-5′TCCTCCG CTTATTGATATGC3′ [18]. A single discrete PCR amplicon band was observed when resolved on agarose gel. The PCR amplicon was purified to remove contaminants. Forward and reverse DNA sequencing reaction of the PCR amplicon was carried out with 27F/1492R primers for bacteria, and then 35 amplification cycles at 94°C for 45 s, 55°C for 60 s, and 72°C for 60 s were performed using a Big Dye terminator cycle sequencing kit (Applied BioSystems, USA). Sequencing products were resolved on an Applied Bio-systems model 3730XL automated DNA sequencing system (Applied BioSystems, USA). Data were submitted to the Gene Bank database. The DNA sequence was compared with the Gene Bank database in the national Centre for Biotechnology Information (http: //www.ncbi.nlm.nih.gov) using the BLAST program [19].

Production and isolation of EPS

Inoculums were prepared by transferring one loopful of NRC-47 culture from marine nutrient slant to an Erlenmeyer flask (250 ml) containing 50 ml seed medium containing (g/l) glucose, 20; yeast extract, 0.1; $CaCO_3$, 1; NH_4NO_3, 0.8; K_2HPSO_4, 0.6; KH_2PO_4, 0.5; $MgSO_4.7H_2O$, 0.05 and $MnSO_4.4H_2O$, 0.1 in 75% seawater [20]. The seed culture was grown at 37°C on a rotary shaker incubator at 150 rpm for 18 h. After incubation, 3 ml of the seed culture was transferred into an Erlenmeyer flask (250 ml) containing 50 ml of fermentation medium (g/l) sucrose, 20; tryptose, 0.7; $MgSO_4.7H_2O$, 0.5; $MnSO_4.4H_2O$, 0.05, $FeSO_4.7H_2O$, 0.01 and $CaCl_2.2H_2O$, 0.01 in 75% seawater pH 7.0 [21]. The fermentation culture was then incubated at 37°C with shaking at 150 rpm for 3 days. Crude broth was centrifuged at 5000 rpm for 30 min. The supernatant was dialyzed three times (1000 ml × 3) against flowing tapwater using dialysis tubing (MWCO 2000) for 48 h. The solution was dialyzed through precipitation with 3 volume chilled ethanol, then the precipitate was washed by acetone, diethyl ether and dried at 60°C until constant weight. Crude polysaccharide was fractionated and purified by anion-exchange chromatography. The crude polysaccharide (300 mg) was dissolved in 10 ml distilled water, and loaded on the diethylaminoethyl (DEAE) cellulose 52 columns (2.5 × 50 cm, i.d). The column was eluted with distilled water, followed by a 0.0–2.0 mol/l linear gradient of NaCl at a flow rate of 0.6 ml/min. The elution of polysaccharide was monitored using a phenol–sulfuric acid assay [15]. The main fraction containing polysaccharide was pooled, dialyzed and then lyophilized for further investigation.

Chemical analysis

The purified AXEPS (50 mg) was subjected to hydrolysis with 6N HCl for 4 h at 100°C in a sealed tube. Excess acid was removed by evaporation on a water bath at a temperature of 40°C and co-distilled with water (1 ml × 3) [22]. Uronic acid contents were determined by measuring the absorbance at 525 nm using the *m*-hydroxybiphenyl colorimetric procedure and with glucuronic acid as the standard [23]. Sulfate was measured using the turbidimetric method [24], with sodium sulfate as standard. N-acetyl glucose amine was estimated by the Elson–Morgan reaction [25]. Monosaccharide composition of the AXEPS was determined by high-performance liquid chromatography (HPLC) on a Shimadzu Shim-Pack SCR-101N column (7.9 mm × 30 cm, i.d.), using deionized water as the mobile phase (flow rate 0.5 ml/min), as described by El-Sayed *et al.* [26].

Determination of molecular weight

The molecular weight of AXEPS was determined on an Agilent 1100 HPLC system equipped with a refractive index detector (RID) and FPl gel particle size (5 μm), 3 columns of pore type (100, 104, 105 A°) on series, length 7.5 × 300 mm (1000, 5 000 000) for DMF solvent Styrogel HR-DMF, 3 μm (7.8 × 300 mm), Water Company Ireland. One column (5000–600 000) for water solvent (polyethylene oxide/glycol standard) PL aquagel-OH 7.5 mm and 30 μm pore type 8 μm particle size, PL aquagel-OH 7.5 mm, 50 μm pore type, 8um particle size, in series Mw from 100–1 250 000 g/mol. The sample 0.01 gm was dissolved in 2 ml of solvent and filtrated by filter 0.45 then the sample was put in a GPC device [27]. The polydispersity index was calculated from the Mw/Mn ratio [28]. Number average molecular weight (Mn) and weight average molecular weight (Mw) were directly calculated according to the definition of Mn and Mw using molecular weight and RI signal values at each elution volume [28].

Spectral analysis

Fourier-transform infrared (FTIR) spectra were recorded from the samples in the KBr pellet on a FTIR spectrophotometer (Bucker scientific 500-IR). The AXEPS was mixed with KBr powder, then ground and pressed into 1-mm pellets for FTIR spectroscopy measurements in the range of 400–4000 cm^{-1} [29]. Ultraviolet–Visible (UV–Vis) spectroscopy analyses were conducted on a UV–Vis–Near-Infrared spectrophotometer 2401PC (Shimadzu, Japan). The polysaccharide solution was prepared by suspending the sample in distilled water to a concentration of 1.0 mg/ml for UV–Vis measurement in the wavelength range of 190–700 nm.

Radical scavenging activity (RSA) of AXEPS

The free-radical scavenging activity of AXEPS was measured against 1,1-diphenyl-2-picryl-hydrazyl (DPPH) radicals using the method of Asker *et al.* [30]. An aliquot of 5 ml of DPPH ethanol solution (freshly prepared at a concentration of 0.1 mmol/l) was added to 1 ml of AXEPS solution in the various concentrations. The mixture was mixed vigorously and incubated at room temperature in the dark for 30 min. Then, the absorbance value of the supernatant was measured at 517 nm after centrifugation at 5000 rpm for 10 min. Lower absorbance of the reaction mixture indicated higher free radical scavenging activity, which was analyzed from the graph (inhibition percentage plotted against concentration of compound). The experiment was carried out in triplicate and averaged. The capability of scavenging the DPPH radical was calculated using the following equation:

$$\text{Scavenging ability}(\%) = [(\Delta A_{517\text{ of control}} - \Delta A_{517\text{ of sample}})/\Delta A_{517\text{ of control}}] \times 100.$$

In vivo experiments

Animals

The study was conducted according to the ethical guidelines (local ethical committee for animal care and use, Egypt). A total of 32 female Sprague–Dawely rats (150–180 g) were obtained from the animal farm of the Egyptian Holding Company for Biological Products and Vaccines, Egypt. Rats were housed in an air-conditioned atmosphere, at a temperature of 25°C with alternatively 12-h light and dark cycles. Animals were acclimated for 2 weeks before experimentation. They were kept on a standard diet and water *ad libitum*.

Ethics statement

The animal treatment protocol was approved by the Animal Care Committee of the National Center for Radiation Research and Technology (NCRRT), Cairo, Egypt. Marine sediment samples (5 g) were collected from Sidi Bisher (Alexandria, Egypt). This location has a species of marine sediments, which bear the harsh environmental conditions and become a privileged to work on them. We confirm that the field studies did not involve endangered or protected species.

Gamma-radiation

Whole-body γ-irradiation was carried out using a cesium (^{137}Cs) source, the Gamma Cell-40 biological irradiator at the National Centre for Radiation Research and Technology (NCRRT), Cairo, Egypt. The animals were exposed to a single dose of (5 Gy) γ-rays with a dose rate of 0.467 Gy/min.

Experimental design

The animals were divided into four groups (eight animals per group) and treated for one week as follows; the first group (GI), acting as a control, received saline (0.5 ml/100 g body weight (BW)) orally once daily for 4 weeks. The second group (GII) received AXEPS (100 mg/kg BW) orally and daily by oral gavage for four weeks. The third group (GIII) received saline (0.5 ml/100 g BW) for 2 weeks and were then exposed to whole body γ-radiation (5 Gy) and kept for the following 15 days without treatment. The fourth group (GIV) was administered AXEPS (100 mg/kg) as for the second group, but after two weeks, was exposed to single-dose whole-body irradiation (5 Gy) then from 24 h post γ-rays they received AXEPS (100 mg/kg), with that treatment continuing for 15 days after the whole-body γ-radiation (i.e. till the end of the experiment). The fourth group was exposed to γ-rays 24 h after the last dose of AXEPS.

Pharmacological study acute toxicity testing

Determination of acute toxicity (LD_{50}) was carried out using the method of Lorke (1983). A total of 18 rats were used for acute toxicity testing for the determination of $LD_{50/50}$ in two phases nine rats in each phase [31]. In the initial phase, the rats were divided into three groups of three rats each. They were orally treated with 10, 100 and 1000 mg/kg of the extract orally. The rats were observed for 24 h for any mortality. In the second phase, the rats were grouped into three of three rats each and orally treated with the extract at varying doses (1600, 2900 and 5000 mg/kg). The animals were observed for 24 h, and the final LD_{50} value was determined from the minimum concentration (full death) and maximum concentration (no death) of the dose:

$$LD_{50} = (M_0 + M_1)/2,$$

where M_0 = Highest dose of test substance that gave no mortality,

M_1 = Lowest lowest dose of test substance that gave mortality.

Collection of blood and tissue samples

At the end of the fourth week, blood samples were collected from all groups by cardiac puncture into heparin-coated and dry tubes. The blood samples collected were centrifuged at 3000 rpm for 30 min for the separation of plasma and sera. The lower erythrocyte layer in the heparinized tubes was washed three times with phosphate-buffered saline and diluted with an equal volume of the indicated solution. Hematological parameters (total white and red blood cells, hemoglobin concentration, platelet count and PCV percentage) were determined using the Sysmex (Automated Hematology Analyzer Kx-2IN, Sysmex Corporation, Kobe-Japan). It employs a WBC detector block and a WBC/HGB lyse reagent to measure the WBC count and hemoglobin concentration as described [32]. The CD8+ cell count was estimated using a Partec Cyflow Counter, Germany [33].

Determination of CD8+ T lymphocytes

A FACS caliber flow cytometer was used (Becton Dickinson, Sunnyvale, CA, USA) equipped with a compact air-cooled low-power 15-mW Argon ion laser beam (488 nm). The average number of evaluated nuclei per specimen 20 000 and the number of nuclei scanned were 120 s^{-1}. The CD8+ histogram was obtained by a mathematical analysis according to as described by Dean and Jett [34].

Chemotaxis assay

Chemotaxis was determined using the agarose assay [35]. Briefly, three sets of three wells (2.5 mm in diameter and 2.5 mm apart) were cut in an agarose gel (Indubiose A 37). A polymorphonuclear neutrophil suspension (5 µl; corresponding to 5×10^5 cells) was placed in each central well; 5 µl of chemotactic factor (fMet-Leu-Phe, 0.1 µM) was placed in each outer well, and 5 µl of Hanks medium in each inner well. The plates were incubated at 37°C (5% CO_2) for 90 min. Migration was measured as the distance between the border of the middle well and the leading edge in the direction of the chemoattractant well (directed migration or chemotaxis) or the control well (random migration). Results are expressed as the ratio of chemotaxis to random migration (no units).

TNF-α and caspase-3

An enzyme-linked immunosorbent assay kit was used to determine rat tumor necrosis factor alpha (TNF-α) and caspase-3.

Lymphocyte transformation assay

Estimation of lymphocyte transformation index (LT) was carried out to evaluate the cellular immune response, using concanavaline – A (Con-A) cell mitogen (10 µg/ml). Isolated lymphocytes were set into a 96-well tissue culture plate. The first row of wells was left free as the blank (culture medium only), and each of the other wells received 100 µl of treated lymphocyte culture suspension (10^6 lymphocytes/ml) with 50 µl of Con-A. The culture plate was incubated for 48 h at 37°C in a humid an incubator (5% CO_2). After 48 h, MTT dye [3-(4, 5-dimethylthiazol-2)-2, 5-diphenyl tetrazolium bromide] was added in the ratio of 1:10 of the total sample then incubated at 37°C for 4 h. After incubation, 50 µl of lysing buffer (2.5 ml H_2SO_4 and 25 g sodium dodecyl sulfate /250 ml distilled water) was added and the solution was then incubated overnight. Optical density was recorded at 470 nm using an ELISA reader (Dynalink, USA) to estimate the LT. The difference inoptical density readings between the treated and control samples were subjected to statistical analysis [36, 37].

DNA in bone marrow was determined by comet assay

The comet assay was performed as described by Singh *et al.* [38]. The femurs were removed, and the bone marrow at both ends was exposed with bone cutters. Cells were flushed out with 3 ml phosphate-buffered saline (PBS) using a needle and syringe, and the cell suspension was filtered through a 150-µm bolting cloth. The cell suspension (25 µl) was mixed 1:10 with 250 µl molten low-melting-point (LMP) agarose, and samples of 75 µl of the mixture were rapidly spread on comet slides. After gelling for 20 min at 4°C in the dark, slides were put in a tank filled with lysis solution (2.5 M NaCl, 0.1 M EDTA, 10 mM Tris base, 1% sodium lauroyl sarcosinate and 1% Triton X-100) for 1 h at 4°C in the dark. Slides were then washed three times with neutralization buffer (0.4 M Tris, pH 7.5) for 5 min and incubated in the fresh alkaline buffer (0.3 M NaOH and 1 mM EDTA, pH >13) for 30 min at room temperature to allow unwinding of DNA. Electrophoresis was then carried out at room temperature in the fresh ice-cold alkaline electrophoresis buffer for 30 min (1V/cm; 300 mA). After electrophoresis, slides were gently washed three times for 5 min in fresh neutralization buffer and exposed to 70% ethanol for 5 min. After drying at room temperature, slides were stained with 25 µl of ethidium bromide solution (20 µg/ml) and covered with a coverslip. Comets were examined at ×200 magnification using fluorescence microscope by Nikon CLIPSE TE2000-S and Nikon Digital Sight DS-U1. The quantification of the DNA strand breaks of the stored images was performed using CASP software, from which the percentage of DNA in the tail, tail length, and tail moment could be obtained directly.

Statistical analysis

The parameter values were all expressed as the mean ± SEM. Significant differences between the groups were determined by one-way analysis of variance (ANOVA) followed by Tukey's multiple comparison tests using SPSS 22.0 software package program. The results were considered significant if $P < 0.05$.

RESULTS

In vitro experiment

Screening and identification of the strain

A total of 40 bacterial strains were isolated from the marine sediment. It was selected fifteen strains on the basis of the colonies form and amount of carbohydrates in an environment fermentation. Most of the isolates could produce EPSs, but strain NRC-47 was selected for further study because of having the highest EPS production capability (5 g l^{-1}). The cells were an aerobic, motile, gram-negative, rod-shaped that is a non-fermenting and catalase and oxidase positive. The strain produced amylase, arginine dihydrolase and penicillinase and was positive for nitrate reduction, the Voges–Proskauer test and acid production from glucose, but negative for gas production from glucose [4]. The partially sequenced 16S rRNA gene (814 bp) was identified and deposited in Gene Bank at NCBI (http://www.ncbi.nlm.nih. gov/nuccore/JQ425073) with the accession number KP145015. BLAST analysis revealed that NRC-47 belonged to the genus *Alcaligenes* and demonstrated a high similarity of 99% with

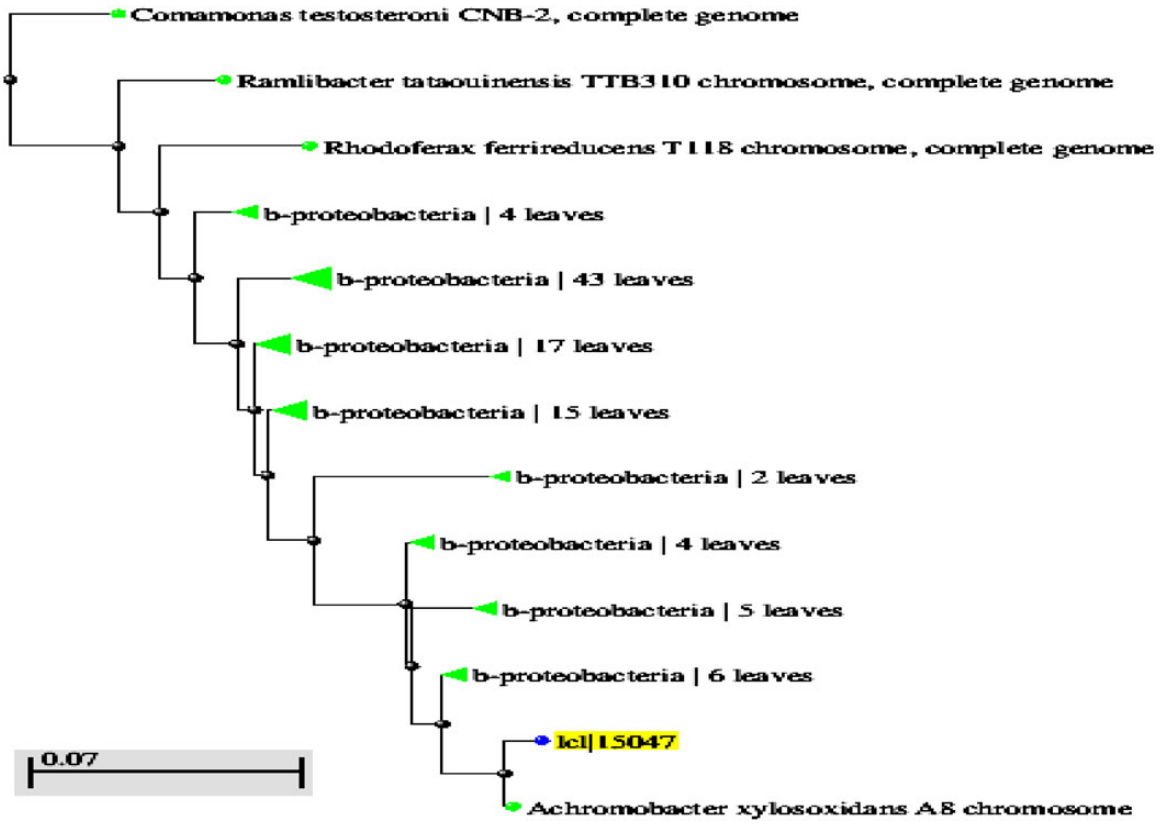

Fig. 1. Phylogenetic neighbor-joining tree obtained from the 16S rDNA sequences of strain NRC-47 and members of related bacteria. Numbers at branch points are bootstrap values for parsimony-based analysis.

Alcaligenes xylosoxidans. A neighbor-joining dentrogram was constructed for the phytogenetic analysis of this bacterium, as shown in Fig. 1. Some EPS-producing marine strains have been studied, which has led to the discovery and isolation of novel macromolecules [39]. Marine bacterial EPSs have been the subject of some reviews [40].

Preparation and physicochemical characteristics of AXEPS

When cultured in the production medium at 37°C for 72 h, *A. xylosoxidans* MSA3 produced a large amount of EPS. Crude EPS (5.4 g l^{-1}) was obtained from fermented broth by ethanol precipitation and dehydration *in vacuo*. Purified AXEPS was obtained from crude EPS by a sequential purification process (Fig. 2). The purified AXEPS, a creamy powder, was used for subsequent analysis. It had a positive response to the Bradford test and an absorption at 280 nm in the UV spectrum, indicating the present of protein and/or amino sugars. As determined by the *m*-hydroxydiphenyl colorimetric method, the polysaccharide contained uronic acid. These characteristics indicate that the AXEPS is an acidic polysaccharide. The weight-average molecular weight (Mw), number-average molecular weight and the polydispersity (PI) of AXEPS were calculated by GPC. The AXEPS in the GPC chromatogram (Fig. 3) had a widely dispersed molecules polydispersity index (Mw/Mn = 2.8; the ratio of weight average molecular weight to number average molecular weight) and had an overall weight average molecular weight (Mw) of 1.6 $\times 10^4$ g mol^{-1} and number average molecular weight (Mn) of 5.7 $\times 10^3$ g mol^{-1}. The bioactivities of EPS seemed to be also affected by its molecular

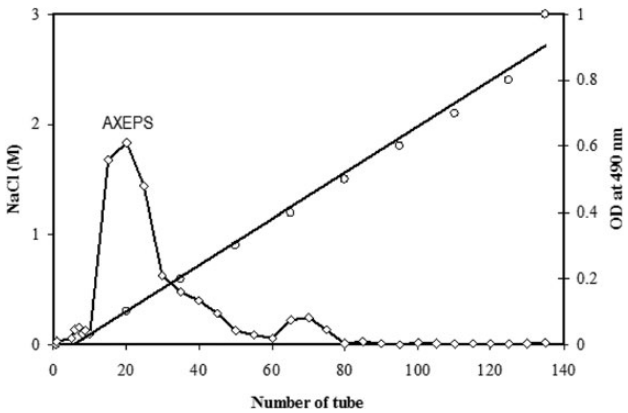

Fig. 2. Elution curve of AXEPS from *Alcaligenes xylosoxidans* MSA3 over DEAE-cellulose column. The absorbance at 490 nm was that of the resulting reactive solutions of polysaccharides, phenol and sulfuric acid.

weight. It was shown that the low molecular weight of the EPS from *Bifidobacterium animalis* RH possibly resulted in its strong antioxidant activity [41]. A high molecular weight EPS seemed to inhibit metastasis of the rat mammary adenocarcinoma [42]. AXEPS contained 30% uronic acid, as evaluated by the *m*-hydroxydiphenyl colorimetric method, 7.3% sulfate 4.9% and N-acetyl glucose amine. Xu *et al.* [43] reported that WTF-B, a water-soluble homogeneous polysaccharide

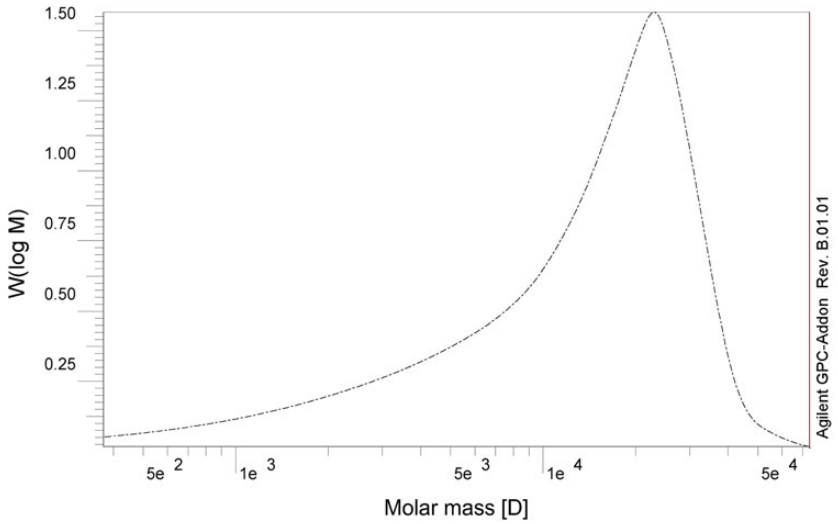

Fig. 3. Molecular weight distributions of AXEPS production by *Alcaligenes xylosoxidans* MSA3.

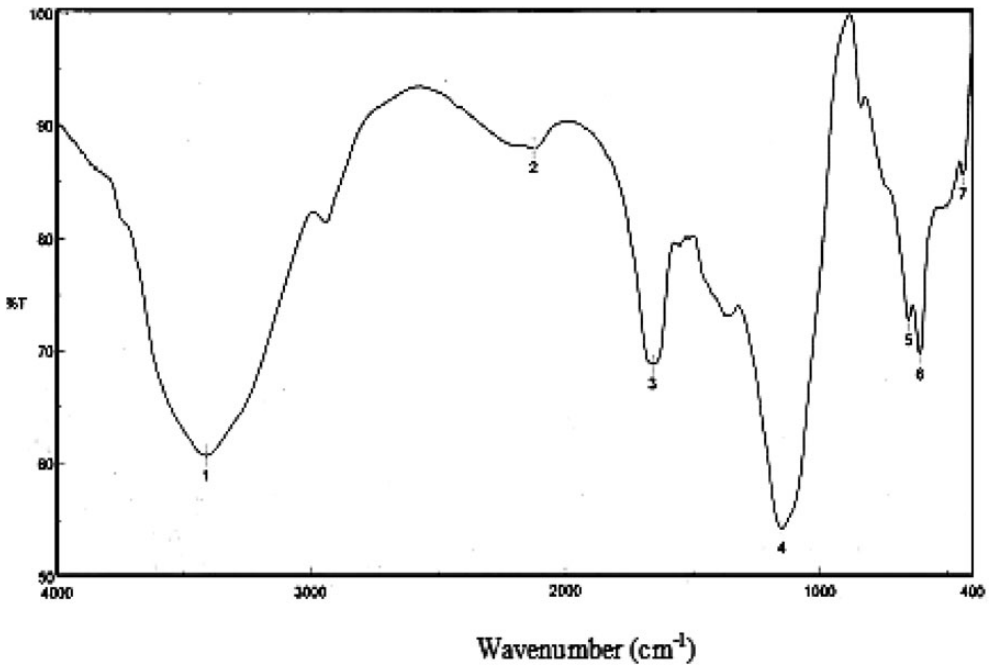

Fig. 4. FT–IR spectrum of the AXEPS from *Alcaligenes xylosoxidans* MSA3 in the range 400–4000 cm^{-1}.

from *Tremella fuciformis*, contained 32.88% uronic acid and used radiation-induced damage in mice. Analysis by HPLC indicated that AXEPS was composed of glucose, galactose, rhamnose and glucuronic acid in a molar ratio of ~1.0:1.6:0.4:2.3, respectively. The chemical composition and molecular weight of polysaccharides from microorganisms depend on the kind of microorganism, the environmental conditions and the location of the isolate. The FTIR spectrum of AXEPS is shown in (Fig. 4). A characteristic great medium N-H stretching peak around 3336 cm^{-1} (for the amines and amides group) and a medium band at 2923 cm^{-1} (showing the C-H stretching and alkenes group) were observed. The peaks of 1147 and 1055 cm^{-1} corresponded to the aliphatic amines group medium C-N stretch [44]; a stretching peak appeared at 1660 cm^{-1} and a weak stretching peaks at 1420 cm^{-1} and 1351 cm^{-1}, suggesting the presence of carboxyl groups. The absorption at 1147cm^{-1} could be attributed to the presence of sulfate groups in the form of S = O and C–O–S [45]. Moreover, the characteristic absorption at 850 cm^{-1} in the IR spectra indicated that α-configurations were simultaneously present in AXEPS [46, 47]. The largest absorbance peak of AXEPS was 197 nm, which revealed characteristics of polysaccharide. There was weak absorption at 280 nm in AXEPS, indicating that it contained very small amounts of NH_4^+ groups in the polysaccharide.

Antioxidant activity of AXEPS

Natural antioxidants play important protective roles against various diseases and aging processes due to their capability of scavenging free radicals and binding transition metal ion catalysts as well as their reductive activity and ability to prevent chain initiation. It is well known that ROS (such as hydroxyl radicals, superoxide anion and hydrogen peroxide) are related to the pathogenesis of various diseases [48]. The *in vitro* antioxidant activity of the AXEPS was determined by assays to determine its scavenging abilities on DPPH radicals, and these abilities were compared with those of ascorbic acid (Vc). As shown in Fig. 5, the scavenging activities of both AXEPS and Vc on DPPH radicals acted in a concentration-dependent manner with an IC50 value of 0.5 mg/ml. Under the same conditions, Vc, a free-radical scavenger, showed a stronger effect on the hydroxyl radicals, with an IC50 value of 0.3 mg/ml. These results indicated that AXEPS had a noticeable effect on scavenging free radicals, especially at a high concentration.

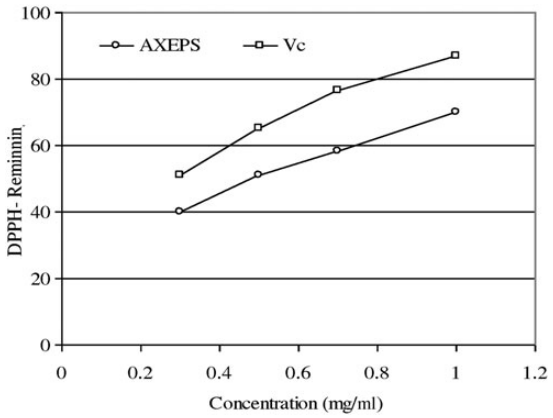

Fig. 5. Scavenging effect of polysaccharide fraction AXEPS during DPPH test and measured by changes in absorbance at 517 nm.

II- Biological activities of AXEPS: in vivo

The data presented in Table 1 indicate a significant decrease in the hematological constituents of peripheral blood [platelet (PLT) count, hemoglobin (Hb), white blood cell (WBC) count, red blood cell (RB) count, and packed-cell volume (PCV) percentages] in rats exposed to γ-radiation alone. While AXEPS-treated Groups II and IV showed a significant increase ($P < 0.05$) in the hematological constituents when compared with an irradiated group (III), the results presented in Table 2 indicate there were significant decreases in CD8+ and in the chemotactic index in rats exposed to γ-radiation alone (13.995 ± 1.74 and 1.31 ± 0.02, respectively). AXEPS administered for 14 days before exposure to γ-radiation and after was associated with a significant increase (21.80±1.66 and 1.54± 0.04, respectively,

Table 1. Effect of AXEPS on the hematological constituents in irradiated rats

Groups	Normal (GI)	AXEPS (GII)	Irradiated (GIII)	Treatment with AXEPS (GIV)	*F* value
Hb (g/dl)	12.39 ± 0.32^{a}	13.41 ± 0.69^{a}	9.69 ± 0.41^{b}	12.45 ± 11.60^{a}	10.852*
PL (PLTC/C mm)	588.50 ± 37.9^{a}	591.25 ± 31.54^{a}	394.50 ± 24.13^{b}	566.50 ± 36.88^{a}	7.310*
WBCs (cells × 10^3/mm)	12.87 ± 0.12^{a}	12.58 ± 0.23^{a}	9.55 ± 0.63^{b}	11.82 ± 0.70^{a}	8.039*
RBCs (cells × 10^6/mm)	6.35 ± 0.45^{a}	6.44 ± 0.30^{a}	4.82 ± 0.18^{b}	5.99 ± 0.51^{ab}	2.83†
PCV (%)	39.79 ± 2.10^{a}	37.65 ± 1.19^{a}	27.10 ± 1.27^{b}	36.25 ± 1.93a	7.578*

Data expressed as mean ± SE. a,b and ab: Statistically significant from control or radiation group, respectively at $P < 0.05$ using one-way ANOVA followed by Tukey–Kramer as a *post hoc* test. *F value ($P < 0.05$); † $P = 0.668$ ($P > 0.05$).

Table 2. Effect of AXEPS on CD8+ T, caspase-3, TNF-α, chemotactic index and LT in irradiated rats

Groups	Normal (GI)	AXEPS (GII)	Irradiated (GIII)	Treatment with AXEPS (GIV)	*F* value
CD8+ T (%)	22.84 ± 1.21^{a}	21.45 ± 0.93^{a}	13.99 ± 1.74^{b}	21.80 ± 1.66^{a}	6.76*
Caspase3 (ng/ml)	3.44 ± 0.11^{b}	3.36 ± 0.15^{b}	5.66 ± 0.08^{a}	3.45 ± 0.28^{b}	16.699*
TNF-α (pg/ml)	81.90 ± 6.26^{c}	78.09 ± 1.13^{c}	120.33 ± 2.64^{a}	98.19 ± 1.73^{b}	54.255*
Chemotactic-index	1.60 ± 0.01^{b}	1.87 ± 0.03^{a}	1.31 ± 0.02^{c}	1.54 ± 0.04^{b}	43.56*
LT	1.73 ± 0.10^{b}	1.92 ± 0.12^{ab}	2.44 ± 0.37^{a}	1.65 ± 0.14^{b}	3.02†

Data expressed as mean ± SE. a, b, ab and c: statistically significant from control or radiation group, respectively at $P < 0.05$ using one-way ANOVA test followed by Tukey–Kramer test as a *post hoc* test. *F value ($P < 0.05$); † ($P > 0.05$).

$P < 0.05$) in the CD8+ level and Chemotactic-index (Table 2). Nevertheless, the chemotactic index indicated a significant alteration in Group IV (AXEPS before and after administration) by the end of the experiment, but it remained higher than in the normal control group (Group I) (Table 2). In the present study, whole-body γ-rays induced a significant increase in LT, TNF-α and caspase-3 compared with normal control rats (Table 2). AXEPS-treated Groups II and IV animals showed a significant ($P < 0.05$) decrease in LT, and caspase-3 reached within a normal level; at the same time, TNF-α showed a significant decrease in the groups with either AXEPS alone or both before and after whole-body γ-radiation by the end of the experiment, although in Group IV the level was still higher than in the normal control (Table 2). Three parameters were adopted as indicators of DNA damage: tail length (TL; tail length of DNA migration), tail moment (TM) and tail damage DNA (related directly to the DNA fragment size and given in micrometers). It was calculated from the centre of the cell. The percent of DNA in the comet tail (% tail DNA), which is an estimate of DNA damage and TM, was calculated from the product of the TL and the fraction of DNA in the comet tail. The comet assay revealed that whole-body γ-ray exposure induced a statistically significant ($P < 0.05$) increase in the mean value of the TL and TM (from 1.78 ± 0.43 and 2.78 ± 0.61, respectively, in the control group to 4.92 ± 0.41 and 16.33 ± 0.96, respectively). A significant increase in the % tail DNA was seen in the nuclei of bone marrow from whole-body γ-ray-irradiated rats, as compared with those of saline-treated animals ($P < 0.05$). In Group IV, a significant decrease was found in the % tail DNA damage in animals treated with AXEPS (100 BW) 24-h-post whole-body γ-radiation as compared with that in γ-radiation-treated animals alone ($P < 0.05$; Table 3 and Fig. 6).

The oral LD50 study of the extract in rats was found to be >300 mg/kg (Table 4). No toxicity effects or mortality were observed in rats when EPS was administered at 100 mg/kg BW throughout the experimental period.

Table 3. Effect of AXEPS on genomic DNA in irradiated rats

Groups	Normal (GI)	AXEPS (GII)	Irradiated (GIII)	Treatment with AXEPS (GIV)	*F* value
Tail DNA (%)	1.57 ± 0.04^{c}	2.65 ± 0.27^{b}	3.39 ± 0.42^{a}	3.15 ± 0.08^{ab}	9.148*
Untailed (%)	95.50 ± 0.88^{a}	95.33 ± 0.9^{a}	81.33 ± 0.67^{c}	86.33 ± 0.88^{b}	71.133*
Tail length (μm)	1.78 ± 0.43^{c}	1.31 ± 0.14^{c}	4.92 ± 0.41^{a}	3.00 ± 0.25^{b}	27.594*
Tail moment	2.78 ± 0.61^{c}	3.41 ± 0.21^{c}	16.33 ± 0.96^{b}	9.43 ± 0.57^{b}	101.39*

Data expressed as mean ± SE. a, b, ab, and c: statistically significant from control or radiation group, respectively at $P < 0.05$ using one-way ANOVA test followed by Tukey–Kramer test as a *post hoc* test. *F value ($P < 0.05$).

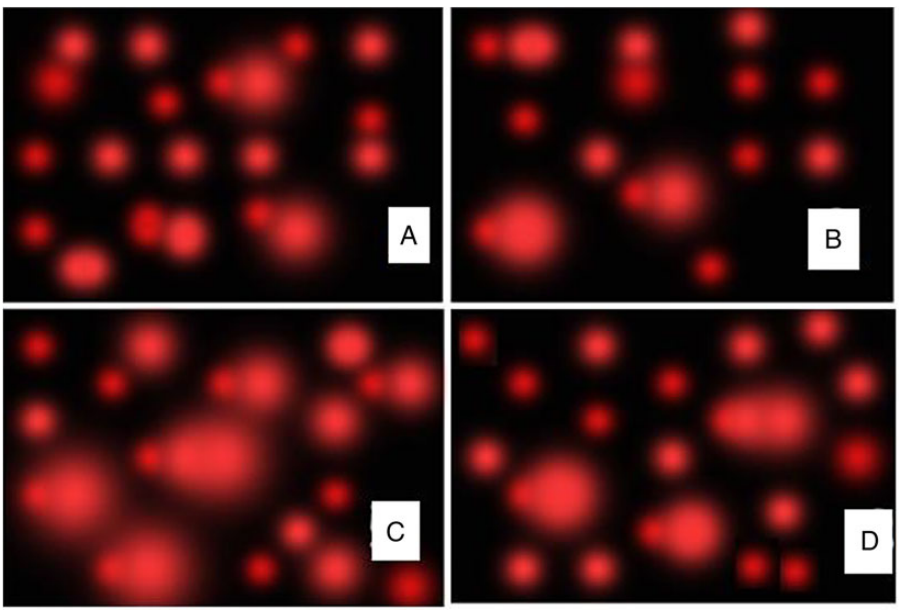

Fig. 6. Effect of AXEPS on genomic DNA in irradiated rats: (A) control; (B) rats treated with AXEPS only; (C) irradiated rats; (D) irradiated rats treated with AXEPS 2 weeks before γ rays and continued till 15 days after γ rays.

Table 4. Pharmacological study of acute toxicity (LD) testing

Doses (mg/kg)	Result of first phase (mortality) $n = 3$
10	0/3
100	0/3
1000	1/3
Doses (mg/kg)	Result of second phase (mortality) $n = 3$
1600	1/3
2900	2/3
5000	3/3

DISCUSSION

The results from the present study indicate that pre and post-treatment with AXEPS protects against radiation-induced hematological and biochemical alterations in rats. The radioprotective effect of polysaccharides isolated was demonstrated by evaluating the hematological parameters such as Hb, total WBCs, RBC counts, PCV% and PLTs post irradiation. Our results revealed that the oral LD50 study of the extract in rats was found to be ≈ 1300 mg/kg. No toxicity effects were observed in mice or rats when EPS was administered in amounts ranging from 20 to 200 mg per kg BW [49]. It was not possible to increase the amount of EPS tested due to its high viscosity and the quantity of material that could be dissolved in water. Increasing the amount of EPS would require a larger volume of solution to be injected. Under these conditions, rats and mice could suffer (or even die) from the large volume of the injection, rather than from the effects of the EPS [50].

In the present study, a significant decrease in the hematological constituents of peripheral blood in animals in the irradiation-only group was observed. The decline in hematological constituents may be attributed to direct damage by radiation. Although, a 5 Gy total body dose is required to produce detectable depletion in total erythrocyte cells, whole-body irradiation in a moderate dose range (5–10 Gy) leads to a decreased concentration of all the cellular elements in the blood. This could be due to direct destruction of mature circulating cells, loss of cells from the circulation by hemorrhage, or leakage through capillary walls and decreased production of cells [51]. Mitotically active precursor cells are sterilized by radiation, and the subsequent supply of RBCs, WBCs and platelets is thereby diminished. On the other hand, irradiated group pre and post treatment with AXEPS showed a significant increase in the hematological parameters compared with the irradiated group. Some investigators have reported alterations in the hematological parameters after exposure to irradiation [52], some of which are in harmony with the present investigation. RBC count and Hb values were depressed post whole-body γ-radiation in the dose-range 5–10 Gy [53, 54]. The depression observed in RBCs, Hb and PLTs could be attributed to destruction of erythrocyte precursors in the bone marrow [54]. Irradiation causes retardation in the incorporation of iron and a decrease in Hb binding to the erythrocyte membrane [55]. The underlying cause of the increased lysing of RBCs by irradiation appears to a decreased production of erythropoietin [56, 57]. These findings indicate that anemia may occur following acute exposure to a single radiation dose. Anemia is a common problem associated with irradiation of a large body area that includes bone marrow [51]. Peslak *et al.* [58] concluded that sublethal radiation injury leads to a marked reduction in reticulocyte output and the subsequent onset of anemia, which provides the stimulus for the rise in endogenous erythropoietin levels. Several studies have suggested that bone marrow progenitors and precursors are directly injured after radiation damage [58]. Significant depression in bone marrow viable cells in irradiated animals is concomitant with these results. Furthermore, recently, the studies found that 4 Gy total-body irradiation (TBI) rapidly induces the apoptosis of bone marrow erythroid progenitors and precursors, leading to severe depletion of bone marrow erythroblasts [59]. Thus, radiation-induced erythroid stress, in which marrow erythroblasts are directly depleted and peripheral red cells relatively preserved, is nearly the opposite of more traditional erythroid stressors, such as bleeding or hemolysis, in which the circulating red cell compartment is rapidly and severely lost but bone marrow erythroblasts are preserved.

Erythrocyte hemolysis is caused by lipid peroxidation [60]. Ionizing γ-irradiation hazards present an enormous challenge for biological and medical safety due to the generation of free radicals [61]. In the present study, whole-body γ-radiation markedly inhibited the production of T cells, represented by the CD8+ count and the chemotactic index; this was ameliorated by AXEPS administration pre and post- γ-radiation treatment, which normalized them. Exposure to IR also enhanced CD8+ production in the thymus and CD8+ T cell production in the spleen [61–63]; the increase in natural killer T cell activity post irradiation, together with a reduction in the percentage of B cells in blood lymphocytes, was concomitant with an increase in the helper T cell population [64]. The ability of cells to migrate directionally in the presence of gradients of chemo-attractants, referred to as 'chemotaxis', is a fundamental physiological response in biology [65]. Exposure to IR induced an additional decrease in chemotaxis immediately after an acute dose in the transition stage of the food-NaCl associative learning [66]. Thus, the IR-induced response would not be a single-time event, but a constitutive activity. This could be a radio-adaptive response, which has been under debate for radiation protection guidelines [67]. Neta [68] assessed percentage of apoptotic lymphocytes induced by irradiation concurs well with the percentage of chemotaxis-impaired cells. The present study revealed a significant increase in TNF-α post irradiation. The role of γ-irradiation in increasing inflammatory resorbing cytokines is well known [69]; however, the increase in serum TNF-α may be strongly linked to osteoclastogenesis [70]. Chemotaxis is crucial for leukocytes to be able to migrate to sites of inflammation and infection, and a large number of chemotactic factors [71] and lipids [72] have been demonstrated to be chemo-attractants. The chemokines can be subdivided into two major families, based on the sequence of the cysteine residues in chemokines [73]. A significant increase in LT was detected in the present study following exposure to γ-irradiation. This data is in accordance with the results of McFarland *et al.* [74], who suggested that TBI of mammals causes generalized immunosuppression, in part by induction of lymphocyte apoptosis. The T lymphocyte subpopulation plays an important role in the T lymphocyte immune function [75]. Our findings indicated that long-term exposure to AXEPS could activate the T lymphocyte immune function. In our research, AXEPS was able to promote the immune

function of erythrocytes in the blood of rats. T lymphocyte immune function was also affected by AXEPS. This experiment highlighted the relationship between AXEPS and T lymphocyte immune function, indicating a possible advantage of supplementation to AXEPS. No deaths occurred in the AXEPS-treated rats during the experimental period. CD8+ T lymphocytes were decreased in the AXEPS-treated rats or cells. So, our results indicated that AXEPS could promote T lymphocyte immune function, partially by increasing the T cell subpopulation. TNF-α was also secreted by macrophages. Both cytokines could modulate the T lymphocyte immune function [75]. Studies on both mice and cells indicated that AXEPS promoted the levels of IL-2 and TNF-α, and levels of IL-2 and TNF-α were increased in an AXEPS-dose-dependent manner. IL-2 and TNF-α interacted: if one increased, the other should increase [76]. In this study, genotoxic effects induced by whole-body γ-irradiation were observed as an increase in the comet assay parameters (TL, % tail DNA and TM) in bone marrow of exposed rats. This data was in accordance with the results of Cao *et al.* [76], who suggested that irradiation induces bone injury by producing free radicals that adversely affect the microenvironment, thus damaging bone marrow blood vessels, which in turn slows bone fracture healing. IR causes free radical–mediated damage in cellular DNA [77]. In the comet assay, AXEPS (100 mg/kg) treatment reduced radiation-induced comets (% tail DNA, tail length and tail moment) compared with radiation only. The decrease in comet parameters is due to the enhanced rate of repair of DNA strand breaks in the tissues of rats administered with AXEPS before and after irradiation.

CONCLUSIONS

The present study is the first to demonstrate the ability of AXEPS to decrease γ-ray radiation-induced cytotoxicity in rats. The protective mechanisms of AXEPS may be attributed to its free-radical scavenging activity and its protective effect against DNA damage. Based on the results obtained, AXEPS can be used for a variety of beneficial chemo-preventive effects. Further studies on the specific components of AXEPS and *in vivo* studies are in progress to understand the detailed mechanism by which AXEPS exerts its radioprotective effect. To conclude, this research confirms that AXEPS has a significant therapeutic potential and also that it is likely to play a role in future scientific discovery and the development of novel compounds of medical value.

ACKNOWLEDGEMENTS

AIH and MAGh contributed to the experimental biology, while MGM, SSM and MSA contributed to the experimental microbiology and chemistry. MGM, SSM and MSA contributed to the study design. All authors took part in planning, designing and supervising the study design, and contributed to the analysis and writing, editing and critical revising of the manuscript with respect to the important intellectual content. All authors read and approved the final manuscript.

FUNDING

Funding to pay the Open Access publication charges for this article was provided by each of the co-authors in this search.

REFERENCES

1. Borek C. Antioxidants and radiation therapy. *J Nutr* 2004;134:3207S–9S.
2. Sun YX, Kennedy JF. Antioxidant activities of different polysaccharide conjugates (CRPs) isolated from the fruiting bodies of *Chroogomphis rutilus* (Schaeff.: Fr.) O. K. Miller. *Carbohydr Polym* 2010;82:510–4.
3. Lemon JA, Rollo CD, Boreham DR. Elevated DNA damage in a mouse model of oxidative stress: impacts of ionizing radiation and a protective dietary supplement. *Mutagenesis* 2008;23:473–82.
4. Weiss JF, Landauer MR. Protection against ionizing radiation by antioxidant nutrients and phytochemicals. *Toxicology* 2003;189:13–20.
5. Mateos-Aparicio I, Mateos-Peinado C, Jiménez-Escrig A, et al. Multifunctional antioxidant activity of polysaccharide fractions from the soybean byproduct okara. *Carbohydr Polym* 2010;82:245–50.
6. Zhang LM. Chemical structural and chain conformational characterization of some bioactive polysaccharides isolated from natural sources. *Carbohydr Polym* 2010;76:349–61.
7. Pillai TG, Krishnan C, Nair CCK, et al. Polysaccharides isolated from *Ganoderma lucidum* occurring in southern parts of India, protects radiation induced damages both *in vitro* and *in vivo*. *Environ Toxicol Pharmacol* 2008;26:80–5.
8. Ni W, Zhang X, Wang B, et al. Antitumor activities and immunomodulatory effects of ginseng neutral polysaccharides in combination with 5-fluorouracil. *J Med Food* 2010;3:270–7.
9. O'Neill MA, Selvendran RR, Morris VJ, et al. Structure of the extracellular polysaccharide produced by the bacterium *Alcaligenes* (ATCC 31555) species. *Carbohydr Res* 1986;145:295–313.
10. Li H, Xu H, Xu H, et al. Optimization of exopolysaccharide welan gum production by *Alcaligenes* sp. CGMCC2428 with Tween-40 using response surface methodology *Carbohydr Polym* 2012;87:1363–8.
11. Chandrasekaran R, Radha A, Lee EJ. Structural roles of calcium ions and side chains in welan: an X-ray study. *Carbohydr Res* 1994;252:183–207.
12. Li S, Xu H, Shi N. Production of a microbial polysaccharides by fermentation. *Food & Ferment. Indus.* 2004;30:6–9.
13. Guo CJ, Qiao HQ, Li S, et al. Breeding of welan gum-producing bacteria by low-energy N^+ ion implantation. *J. of Rad. Res. & Rad. Proce.* 2007;25:266–70.
14. Li S, Xu H, Li H, Guo C. Optimizing the production of welan gum by *Alcaligenes faecalis* NX-3 using statistical experiment design. *Afr J Biotech* 2010;9:1024–30.
15. Dubois M, Gilles KA, Hamilton JK, et al. Colorimetric method for determination of sugars and related substances. *Anal Chem* 1956;28:350–6.
16. Cappuccino JG, Sherman N. *Microbiology: A Laboratory Manual*. New Delhi, India: Pearson Education (Singapore) , 2004.
17. Collins NM, Termites I, Lieth H, et al. *Tropical Rain Forest Ecosystems*. Amsterdam: Elsevier Science Publishers, 1989, 455–71.
18. Weisberg WG, Barns SM, Pelletier BA, et al. 16S ribosomal DNA amplification for phylogenetic study. *J Bacteriol* 1991;173:697–703.
19. Tamura K, Peterson D, Peterson N, et al. Molecular evolutionary genetics analysis using maximum likelihood, evolutionary

distance, and maximum parsimony methods. *Mol Biol Evol* 2011; 28:2731–9.
20. Kim CA, Choi HJ, Kim CB, et al. Drag reduction characteristics of polysaccharide xanthan gum. *Macromol Rapid Commun* 1998;19:419–22.
21. Read RR, Costerton JW. Purification and characterization of adhesive exopolysaccharides from *Pseudomonas putida* and *Pseudomonas fluorescens*. *Can J Microbiol* 1987;33:1080.
22. Sudhamani SR, Tharanathan RN, Prasad MS. Isolation and characterization of an extracellular polysaccharide from *Pseudomonas caryophylli* CFR1705. *Carbohydr polym* 2004;56:423–7.
23. Filisetti-Cozzi TMCC, Carpita NC. Measurement of uronic acids without interference from neutral sugars. *Anal Biochem* 1991; 197:157–62.
24. Dogson KS, Price RG. A note on the determination of the ester sulphate content of 618 sulphated polysaccharides. *Biochem J* 1962;84:106–10.
25. Elson LA, Morgan WTJ. A colorimetric method for the determination of *N*-acetylglucosamine and *N*-acetylchrondrosamine. *Biochem J* 1934;28:988–95.
26. El-Sayed OH, Ismail SA, Ahmed YM, et al. Studies on the production of sulfated polysaccharide by locally isolated bacteria. *Egypt Pharmaceutical J* 2005;4:439–52.
27. Jun L, Jiangguang L, Hong Y, et al. Production, characterization and antioxidant activities *in vitro* of exopolysaccharides from endophytic bacterium *Paenibacillus polymyxa* EJS-3. *Carbohydr Polym* 2009;78:275–81.
28. You L, Gao Q, Feng M, et al. Structural characterisation of polysaccharides from *Tricholoma matsutake* and their antioxidant and antitumour activities. *Food Chem* 2013;138:2242–9.
29. Ray B. Polysaccharides from *Enteromorpha compressa*: isolation, purification and structural features. *Carbohydr Polym* 2006;66: 408–16.
30. Asker MMS, Ahmed YM, Ramadan MF. Chemical characteristics and antioxidant activity of exopolysaccharide fractions from *Microbacterium terregens*. *Carbohydr Polym* 2009;77:563–7.
31. Lorke D. A new approach to practical acute toxicity testing. *Arch Toxicol* 1983;53:275–87.
32. Samuel OI, Thomas N, Ernest OU, et al. Comparison of hematological parameters determined by the Sysmex KX-2IN automated hematology analyzer and the manual count. *BMC Clin Pathol* 2006;10:3–5.
33. Partec Cyflow Counter PCC. *Typical Steps of Particle Analysis Using Partec Cyflow Counter, Instrument Operating Manual*. Munster: Partec GmbH OHO-Hann-str 32, 2010, 5–8.
34. Dean PN, Jett JH. Brief note: mathematical analysis of DNA distributions derived from flow microfluorometry. *J Cell Biol* 1974;60:523–7.
35. Nelson RD, Quie P, Simmons RL. Chemotaxis under agarose: a new and simple method for measuring chemotaxis and spontaneous migration of human polymorphonuclear leukocytes and monocytes. *J Immunol* 1975;115:1650–6.
36. Brulles S, Wells PW. *In vitro* stimulation of avian lymphocytes by various mitogens. *Res Vet Sci* 1977;23:84–6.
37. Rai-el-Balhaa G, Pellerin JL, Bodin G, et al. Importance of the hour of sampling in the lymphoblastic transformation assay of sheep peripheral blood lymphocytes. *Vet Immunol Immunopathol* 1987;16:67–76.
38. Singh NP, McCoy MT, Tice RR, et al. A simple technique for quantitation of low levels of DNA damage in individual cells. *Exp Cell Res* 1988;175:184–91.
39. Finore I, Di Donato P, Mastascusa V, et al. Fermentation technologies for the optimization of marine microbial exopolysaccharide production. *Drugs* 2014;12:3005–24.
40. Xu R, Shen Q, Ding X, et al. Chemical characterization and antioxidant activity of an exopolysaccharide fraction isolated from *Bifidobacterium animalis* RH. *Eur Food Res Technol* 2011;232: 231–40.
41. Pomin VH. Anticoagulant motifs of marine sulfated glycans. *Glyconjugate J* 2014;31:341–4.
42. Parish CR, Coombe DR, Jakobsen KB, et al. Evidence that sulphated polysaccharides inhibit tumour metastasis by blocking tumour-cell-derived heparanases. *Int J Cancer* 1987;40: 511–8.
43. Xu W, Xiu S, Fujun Y, et al. Protective effect of polysaccharides isolated from *Tremella fuciformis* against radiation-induced damage in mice. *J Radiat Res* 2012;53:353–60.
44. Ding X, Feng S, Cao M, et al. Structure characterization of polysaccharide isolated from the fruiting bodies of *Tricholoma matsutake*. *Carbohydr Polym* 2010;81:942–7.
45. Asker MMS, Shawky BT. Structural characterization and antioxidant activity of extracellular polysaccharide isolated from *Brevibacterium otitidis* BTS 44. *Food Chem* 2010;123:315–20.
46. Manivasagan P, Sivasankar P, Venkatesan J, et al. Production and characterization of an extracellular polysaccharide from *Streptomyces violaceus* MM72. *Int J Biol Macromol* 2013;59:29–38.
47. Abe J, Berk BC. Reactive oxygen species as mediators of signal transduction in cardiovascular disease. *Trends Cardiovasc Med* 1988;8:59–64.
48. Begum N, Prasad NR, Thayalan K. Apigenin protects gamma-radiation induced oxidative stress, hematological changes and animal survival in whole body irradiated Swiss albino mice. *Int J Nutr Pharmacol Neurol Dis* 2012;2:45–52.
49. Maeda H, Zhu X, Suzuki S, et al. Structural characterization and biological activities of an exopolysaccharide kefiran produced by *Lactobacillus kefiranofaciens* WT-2B(T). *J Agri Food Chem* 2004;52:5533–8.
50. Sutherland IW. Bacterial exopolysaccharides. In: Kamerling JP (ed.). *Comprehensive Glycoscience*, Vol. 2. Oxford: Elsevier, 2007, 521–57.
51. Ashry OM, Hussein EM. Radio protective potency of Ginseng on some haematopoeilic and physiological parameters in irradiated rats. *Egypt J Rad Sci Applic* 2007;20:46.
52. Alfrey CP, Rice L, Udden MM, et al. Neocytolysis: physiological down-regulator of red-cell mass. *Lancet* 1997;349:1389–90.
53. Saad-El-Din AA, El-Tanahy ZH, El-Sayed SN, et al. Study of electron spin resonance and viscosity for hemoglobin polymers after arsenic trioxide and gamma irradiation treatment. *J Rad Res Appl Sci* 2014;7:448–53.
54. Henke M, Guttenberger R, Barke A, et al. Erythropoietin for patients undergoing radiotherapy: a pilot study. *Radiother Oncol* 1999;50:185–90.

55. Dreval VI, Sichevskaia LV. [Exposure to ionizing radiation decreases haemoglobin binding to erythrocyte membrane]. *Biofizika* 2000;45:1086–8.
56. El-Missiry MA, Fayed TA, El-Sawy MR, et al. Ameliorative effect of melatonin against gamma-irradiation-induced oxidative stress and tissue injury. *Ecotoxicol Environ Saf* 2007;66:278–86.
57. Schwartz GN, Vigneulle RM, MacVittie TJ. Survival of erythroid burst-forming units and erythroid colony-forming units in canine bone marrow cells exposed *in vitro* to 1 MeV neutron radiation or X rays. *Radiat Res* 1986;108:336–47.
58. Peslak SA, Wenger J, Bemis JC, et al. Sublethal radiation injury uncovers a functional transition during erythroid maturation. *Exp Hematol* 2011;39:434–45.
59. Peslak SA, Wenger J, Bemis JC, et al. EPO-mediated expansion of late-stage erythroid progenitors in the bone marrow initiates recovery from sublethal radiation stress. *Blood* 2012;120:2501–11.
60. Ina Y, Sakai K. Activation of immunological network by chronic low-dose-rate irradiation in wild-type mouse strains: analysis of immune cell populations and surface molecules. *Int J Radiat Biol* 2005;81:721–9.
61. Ina Y, Sakai K. Further study on prolongation of life span associated with immunological modification by chronic low-dose-rate irradiation in MRL-lpr/lpr mice: effects of whole-life irradiation. *Radiat Res* 2005;163:418–23.
62. Ina Y, Sakai K. Prolongation of life span associated with immunological modification by chronic low-dose-rate irradiation in MRL-lpr/lpr mice. *Radiat Res* 2004;16:168–73.
63. Kojima S. [Induction of glutathione and activation of immune functions by low-dose, whole-body irradiation with gamma-rays]. *Yakugaku Zasshi* 2006;126:849–57.
64. Ridley AJ, Schwartz MA, Burridge K, et al. Cell migration: integrating signals from front to back. *Science* 2003;302:1704–9.
65. Sakashita T, Hamada N, Ikeda DD, et al. Modulatory effect of ionizing radiation on food–NaCl associative learning: the role of subunit of G protein in *Caenorhabditis elegans*. *FASEB J* 2008;22:713–20.
66. Matsumoto H, Hamada N, Takahashi A, et al. Vanguards of paradigm shift in radiation biology: radiation-induced adaptive and bystander responses. *J Radiat Res* 2007;48:97–106.
67. Wiele C, Philippé J, Van Haelst JP, et al. Relationship of decreased chemotaxis of technetium-99m-HMPAO-labeled lymphocytes to apoptosis. *J Nucl Med* 1997;38:1417–21.
68. Neta R. Modulation of radiation damage by cytokines. *Stem Cells* 1997;15 Suppl 2:87–94.
69. Azuma Y, Kaji K, Katogi R, et al. Stimulation of the ionic transport system in *Brassica napus* by a plant growth-promoting rhizobacterium (*Achromobacter* sp.). *Can J Microbiol* 2000;46:229–36.
70. Hugli TE, Gerard C, Kawahara M, et al. Isolation of three separate anaphylatoxins from complement-activated human serum. *Mol Cell Biochem* 1981;41:59–66.
71. Yokomizo T, Izumi T, Chang K, et al. A G-protein-coupled receptor for leukotriene B4 that mediates chemotaxis. *Nature* 1997;387:620–4.
72. Lodi PJ, Garrett DS, Kuszewski J, et al. Human macrophage inflammatory protein 1 beta. *Science* 1994;263:1762–7.
73. Clore GM, Gronenborn AM. Three-dimensional structures of alpha and beta chemokines. *FASEB J* 1995;9:57–62.
74. McFarland HI, Puig M, Grajkowska LT, et al. Regulatory T cells in γ irradiation-induced immune suppression. *PLoS ONE* 2012;7:e39092.
75. Brunner R, Wallmann J, Szalai K. The impact of aluminium in acid-suppressing drugs on the immune response of BALB/c mice. *Clin Exp Allergy* 2007;37:1566–73.
76. Cao Y, Xu Q, Jin ZD, et al. Induction of adaptive response: preexposure of mice to 900 MHz radiofrequency fields reduces hematopoietic damage caused by subsequent exposure to ionizing radiation. *Int J Radiat Biol* 2011;87:720–8.
77. Ray S, Murmu N, Adhikari J, et al. Inhibition of Hep G2 hepatic cancer *cell* growth and CCl_4 induced liver cytotoxicity in Swiss albino mice by Mahua extract. *J Environ Pathol Toxicol Oncol* 2014;33:295–314.